

## PDF hosted at the Radboud Repository of the Radboud University Nijmegen

The following full text is a publisher's version.

For additional information about this publication click this link.

<http://hdl.handle.net/2066/118479>

Please be advised that this information was generated on 2021-06-22 and may be subject to change.

ARTICLE

Received 24 Oct 2012 | Accepted 7 Jun 2013 | Published 11 Jul 2013

DOI: 10.1038/ncomms3124

OPEN

# Genome evolution predicts genetic interactions in protein complexes and reveals cancer drug targets

Xiaowen Lu<sup>1</sup>, Philip R. Kensche<sup>1</sup>, Martijn A. Huynen<sup>1,2</sup> & Richard A. Notebaart<sup>1,2</sup>

Genetic interactions reveal insights into cellular function and can be used to identify drug targets. Here we construct a new model to predict negative genetic interactions in protein complexes by exploiting the evolutionary history of genes in parallel converging pathways in metabolism. We evaluate our model with protein complexes of *Saccharomyces cerevisiae* and show that the predicted protein pairs more frequently have a negative genetic interaction than random proteins from the same complex. Furthermore, we apply our model to human protein complexes to predict novel cancer drug targets, and identify 20 candidate targets with empirical support and 10 novel targets amenable to further experimental validation. Our study illustrates that negative genetic interactions can be predicted by systematically exploring genome evolution, and that this is useful to identify novel anti-cancer drug targets.

<sup>1</sup>Department of Bioinformatics (CMBI), Centre for Molecular Life Sciences, Radboud University Medical Centre, 6525GA Nijmegen, The Netherlands.

<sup>2</sup>Centre for Systems Biology and Bioenergetics (CSBB), Radboud University Medical Centre, 6525GA Nijmegen, The Netherlands. Correspondence and requests for materials should be addressed to R.A.N. (email: R.notebaart@cmbi.ru.nl).

Knowledge of how proteins interact with each other to exert their function is crucial for understanding how disruption of interactions can lead to disease<sup>1,2</sup> and in the development of treatments. In recent years, several system-level maps of protein complexes have been constructed from physical interaction data<sup>3–5</sup> to initialize understanding of the functional relationships between proteins. These studies are important in identifying which proteins are linked to each other in biological processes<sup>6</sup>. Yet, these maps do not directly reveal how the proteins interact with each other. More specifically, they do not provide information about whether the interaction between two proteins is symmetric, in which both proteins are equally important in the function of a protein complex, or whether the interaction is asymmetric, in which one protein can function in the absence of the other protein, but not *vice versa* (Fig. 1a). One example of such asymmetry is the cyclin–Cdc28 complex where the function of the cyclin, Cln1p, depends on the Cdc28 kinase, but not *vice versa*. The function of Cln1p depends on Cdc28p as transcriptional activation of *CLN1* requires an active Cdc28 kinase<sup>7</sup>. The function of Cdc28p, however, does not depend on

Cln1p as the presence of Cln2p compensates for Cln1p's absence to activate Cdc28p (ref. 8). Thus, there is a functional asymmetry between Cln1p and Cdc28p, where Cln1p depends on Cdc28p and not *vice versa* (Cln1p→Cdc28p). Similarly, there is asymmetry between Cln2p and Cdc28p (Cln2p→Cdc28p). This example shows the relationship between functional asymmetry and what is called a negative genetic interaction, where mutations (for example, knockout) of two genes (for example, *CLN1* and *CLN2*) reduce the fitness much more strongly than would be expected based on the decline in fitness of each gene individually<sup>9</sup>. The concept of negative genetic interactions is very valuable in the development of therapeutic treatments for diseases that can be treated by selectively depleting cells with a disease-causing mutation. Especially promising are the discoveries of cancer drugs that target proteins having synthetic lethal interactions with mutated oncogenes or tumour-suppressor genes<sup>10,11</sup>. The mechanism underlying this treatment is that inhibiting these genes separately is relatively harmless in a normal cell, while it is lethal to a cancer cell as it causes a lethal double mutant with mutated oncogenes/tumour-suppressor genes. Thus, targeting

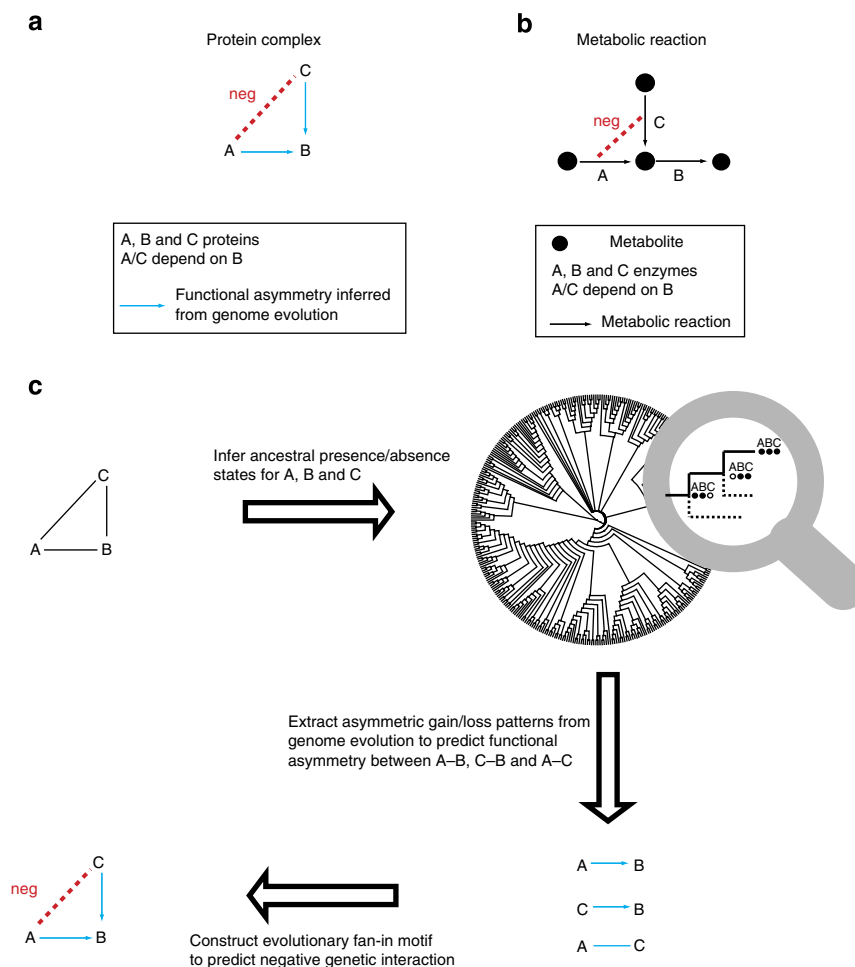


**Figure 1 | Functional asymmetry and negative genetic interactions are linked.** (a) Protein A and B have an asymmetric functional relationship, where the function of A depends on B but not *vice versa*. The asymmetry between protein A and B can be owing to the presence of protein C, which can compensate for a mutant of A. In such a scenario, proteins A and C are predicted to have a negative genetic interaction. (b) Functional asymmetry between enzyme A and B involved in a branched pathway in a metabolic network (A depends on B, but not *vice versa*: A→B). Nodes and arrows represent metabolites and reactions, respectively. The asymmetric relationship is owing to a converging reaction catalysed by enzyme C, which can compensate for A's absence. Thus, enzyme A and C are likely to have a negative genetic interaction. (c) Flowchart to predict negative genetic interactions from genome evolution within a three-member protein complex (protein A, B and C). The blue arrow represents the functional asymmetry between two genes inferred from genome evolution. The blue line represents that there is no evolutionary evidence for a functional asymmetry between two genes. Here, both gene A and C are predicted to have functional asymmetry with B, while gene A and C are predicted not to have functional asymmetry.

these genes can kill the cancer cells while leaving the normal cells relatively unaffected. Prioritizing drug targets in such an approach, by predicting negative genetic interactions between the mutated oncogenes/tumour-suppressor genes and other proteins, is, however, not trivial.

Discovering negative genetic interactions mainly depends on laborious and specific experiments, which can be expensive and time-consuming, partially because of the explosion of the number of pairwise gene combinations. Several computational approaches have been developed to predict genetic interactions by integrating multiple types of functional genomic data, such as synthetic lethality data, physical interaction data and co-expression data<sup>12,13</sup>. These approaches, however, strongly depend on species-specific empirical genetic interaction data as input and therefore do not allow predictions for other species where genetic interaction data are largely unavailable.

Here, we aim to predict negative genetic interactions in protein complexes via the concept of functional asymmetry, which we infer from genome evolution. The example of the cyclin-Cdc28 complex showed that functional asymmetry and negative genetic interaction are linked. This linkage can also be illustrated by enzyme relationships in metabolism. Enzymes in converging pathways have asymmetric relationships with an enzyme in an outgoing pathway<sup>14,15</sup> (Fig. 1b). Consequently, the enzymes in converging pathways can have negative genetic interactions, as they can compensate for each other's absence. Analogous to metabolism, we expect that two proteins in a complex with asymmetry to a third protein will have a negative genetic interaction (Fig. 1a,c). Importantly, the functional asymmetry between enzymes in metabolism is indeed reflected in genome evolution<sup>15,16</sup>.

On the basis of these prior studies, we have developed an evolutionary model to predict asymmetric functional relationships and negative genetic interactions in protein complexes in *S. cerevisiae*<sup>17</sup>. Our model predicts that almost 75% of the protein complexes in *S. cerevisiae* contain functionally asymmetric protein pairs. By integrating the information of predicted asymmetry in protein complexes, we show an up to twofold increase in the predictive power for negative genetic interactions relative to randomly chosen protein pairs from a complex. Moreover, our results show a twofold increase in prediction precision compared with an alternative model<sup>18</sup>. After mapping negative genetic interaction predictions from yeast to human, as well as a direct application to human protein complexes, we predict 20 cancer drug targets with empirical support and 10 completely novel targets not yet experimentally examined. Our study shows that higher-order functional relationships can be predicted by systematically exploring genome evolution, thereby providing a framework to interpret protein complex function with broad application to medical genetics.

## Results

### Functional asymmetry occurs frequently in protein complexes.

In order to examine if patterns in genome evolution can be used to predict negative genetic interactions, we first predicted asymmetry between protein pairs (A–B) in protein complexes from evolutionary analysis. We constructed a model integrating 11 evolutionary variables from the reconstructed ancestral states on a phylogenetic tree of 373 species (Fig. 2 and Methods). For instance, evolutionary asymmetry between proteins A and B is inferred from the occurrence of multiple evolutionary loss events where only one of the two genes was lost in the descendant while both genes were present in the ancestor. If A is more frequently lost than B, then A is expected to be functionally dependent on B (A → B, see Fig. 2a,b, scenario  $f_1$ ). The model was trained on a set

of functionally asymmetric enzyme pairs in the genome-scale metabolic network of *S. cerevisiae*<sup>19</sup> to predict the dependency between the two enzymes (see Methods for detail). Using a tenfold cross-validation, the model showed a correct classification rate of 64.4% and an area under the receiver operator characteristic curve of 0.7 (see Methods for details; Supplementary Fig. S1). It should be noted that the performance of the model becomes worse when using a simpler model with only single gain and loss events (Supplementary Fig. S1). We next asked how frequently functional asymmetry occurs in empirically determined protein complexes from *S. cerevisiae*<sup>17</sup>. Our analysis predicts that 71% (6,145 out of 8,711) of the protein pairs in these protein complexes are functionally asymmetric. Furthermore, ~75% (307 out of 409) of the protein complexes are found to have at least one predicted functionally asymmetric protein pair (Supplementary Fig. S2).

**Empirical evidence for functional asymmetry.** The high frequency of predicted functional asymmetry triggers the question to what extent our predictions are biologically meaningful. To answer this question, we asked whether predicted asymmetry is reflected in genome-scale empirical data. We first examined asymmetry in gene essentiality. For a predicted functionally asymmetric pair (A → B) where only one of the proteins is essential, we expect protein B to be the essential one. To test this, we examined those predicted asymmetric pairs where only one of the encoding proteins is essential and quantified to what extent the predicted asymmetry is consistent with asymmetry in gene essentiality. Our analysis reveals that 72% (1,071 out of 1,497) of the asymmetric pairs (A → B) are consistent with asymmetry in gene essentiality, that is, if one of the two genes is essential, it is B (Fig. 3a; one-tailed Fisher's exact test;  $P < 2.2e - 16$ ).

Many predicted asymmetric pairs have, however, no asymmetry in gene essentiality, simply because the majority of proteins are not strictly essential under standard laboratory conditions (that is, glucose-rich medium)<sup>4</sup>. Approximately 40% of the predicted asymmetric pairs are composed of two non-essential genes. Nevertheless, even when proteins are non-essential they can still contribute to fitness and result in significant growth defects after a gene knockout<sup>20,21</sup>. Similarly to the gene essentiality analysis, we expected that if one of the two proteins in a predicted asymmetric pair (A → B; both non-essential) has a stronger growth defect, it would be protein B. To test this, we examined 511 predicted asymmetric pairs where two non-essential proteins cause different growth defects, and quantified the consistency between the predicted and empirical functional asymmetry. As expected, 63% (322 out of 511) of the cases are consistent (Fig. 3a; one-tailed Fisher's exact test;  $P = 1.40e - 04$ ), that is, the predicted independent protein B has a stronger growth defect when knocked out. This consistency is robust at various cutoffs on empirical growth defect differences (ranging from 0.0001–0.3). Notably, the level of consistency increased from 63 to 67% when we increased the cutoff to 0.3, that is, where growth defect difference is largest. These results show that the evolutionary model is able to capture asymmetric functional relationships in protein complexes. ESCRT-I, a protein complex functioning in cargo selection in the multivesicular body (MVB) sorting pathway, is one example where the predicted functional asymmetry is supported by solid empirical evidence (Fig. 3b).

**Empirical evidence for negative genetic interactions.** An asymmetric functional relationship observed between two proteins A and B can also be linked to a type of relationship known as a negative genetic interaction<sup>9</sup>. The reasoning behind this is that B may not depend on the presence of A, because of the

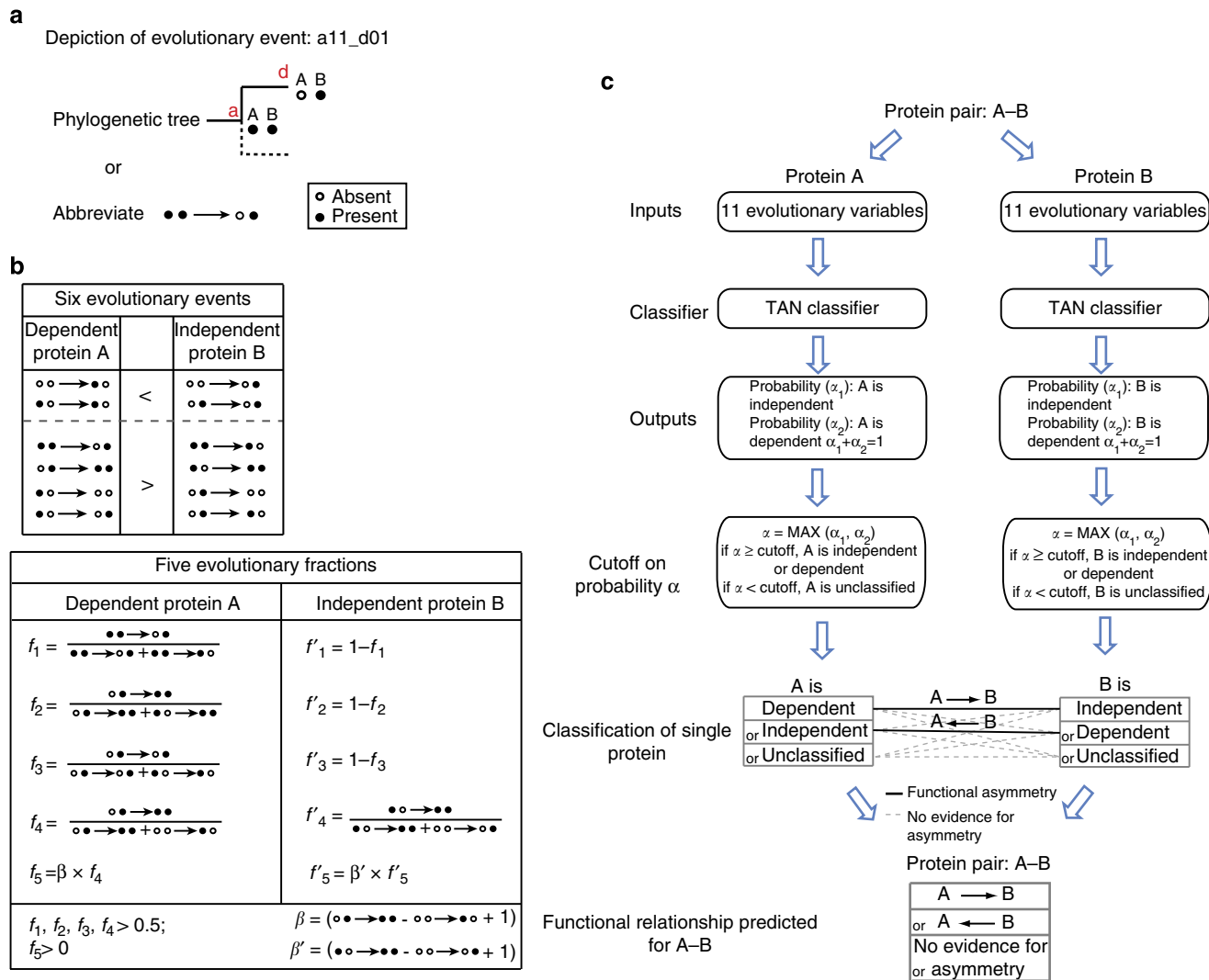


**Figure 2 | Evolutionary variables to predict functional asymmetry.** (a) Depiction of an evolutionary event. It shows a loss of gene A in the descendant (d) when both A and B are present in the ancestor (a). (b) Evolutionary variables used for the Bayesian classifier. The evolutionary variables across history of the dependent protein A in an asymmetric pair (A→B) can be expressed via 11 measures, listed in the first columns of two boxes. Of these 11, 6 count the number of times that a dependent protein A is gained or lost independently of B, including 2 that are expected to occur less often and 4 that are expected to occur more often for a dependent protein than for an independent protein. The remaining five measures are fractions that express relative frequencies of two evolutionary scenarios between A and B.  $f_1, f_2, f_3$  and  $f_4$  are expected to be larger than 0.5;  $f_5$ , that weighs  $f_4$  with the absolute difference between two gain events of A, is expected to be larger than 0. The six evolutionary and the five relative frequencies all contribute to the prediction of functional asymmetry (Supplementary Fig. S1). (c) Schematic presentation of predicting the functional asymmetry in a protein pair (A-B). A TAN classifier was trained on functionally asymmetric enzyme pairs in the metabolic network<sup>14</sup>. For a protein pair (A-B), the 11 evolutionary variables (Fig. 2b) are used to predict the conditional probability that A is functionally independent ( $\alpha_1$ ) or dependent ( $\alpha_2$ ). A is likely to be independent if  $\alpha_1 > \alpha_2$ , or dependent if  $\alpha_1 < \alpha_2$ . Subsequently, A can be predicted as independent, dependent or unclassified by applying a cutoff on probability ( $\alpha = \max(\alpha_1, \alpha_2)$ , see Methods). The same procedure is applied to protein B. By combining the prediction of both, A-B can be either A→B where A is dependent and B is independent, B→A where A is independent and B is dependent, or no evidence for asymmetry when A and B have any other combination of predicted relationship.

presence of another protein C that compensates for A’s absence. We asked whether our evolutionary model is capable of predicting such negative genetic interactions in multi-member protein complexes. We specifically focused on triplets where protein A, B and C are predicted to have an evolutionary fan-in motif (Fig. 1a). This motif is characterized by (i) A and C depend on B, but not *vice versa* and (ii) A does not depend on C and *vice versa*. This motif is analogous to converging pathways in metabolism, in which there is a mechanistic explanation for the compensatory effect between A and C (Fig. 1b). We therefore first investigated to what extent converging metabolic pathways<sup>15,21</sup> show negative genetic interactions<sup>20–28</sup> as a proxy

for compensation, that is, double mutants cause more severe growth defects than expected from the two single mutants. Indeed, enzyme pairs in converging pathways show a threefold enrichment in negative genetic interactions compared with non-converging enzyme pairs (Fig. 3c; one-tailed Fisher’s exact test;  $P = 2.42e - 11$ ).

Given this result, we expect that in cases where we predict a fan-in motif within a protein complex, the A and C proteins have negative genetic interactions with each other. To address this, we compared fan-in A-C pairs with randomly chosen pairs from the same protein complex (that is, non-motif A-C pairs). Our results reveal that the fraction of negative genetic interactions increases

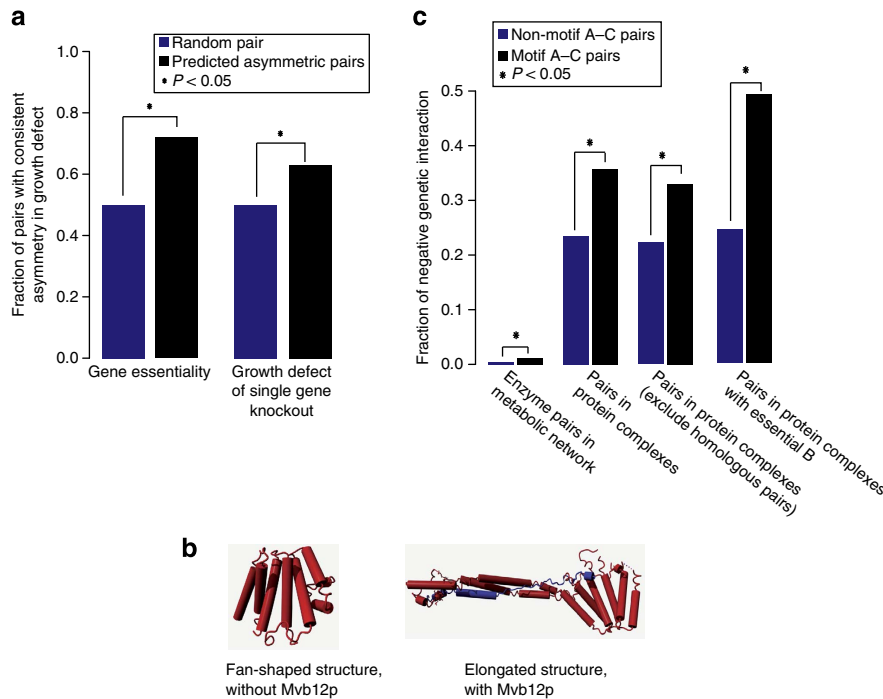


**Figure 3 | Asymmetric functional relationships and negative genetic interactions.** (a) Empirical support for predicted functional asymmetry in gene essentiality<sup>49</sup> and, for non-essential genes, in the growth defect of single-gene knockout<sup>20,21</sup>. For predicted asymmetric pairs ( $A \rightarrow B$ ), the fraction  $f_{AB}$  ( $f_{01} = n_{01}/(n_{01} + n_{10})$ ), where 0 = non-essential or no fitness defect and 1 = essential or substantial growth defect is expected to be larger than 0.5 (fraction in pairs with no asymmetry). (b) One example of predicted functional asymmetry with experimental support. ESCRT-I is composed of four members, Vps23p, Vps28p, Vps37p and Mvb12p. Mvb12p (blue subunit) is predicted to functionally dependent on Vps23p, Vps28p and Vps37p (red) and not vice versa. Structural studies revealed that the functionally dependent subunit, Mvb12p, is a structural stabilizer, which changes the ESCRT-I core complex (Vps23p, Vps28p and Vps37p) from a fan-shaped structure (upper panel) to an elongated structure (lower panel)<sup>57</sup>. First, the dependency of Mvb12 on the core complex is supported by the fact that Mvb12p is unstable in cells lacking any of the other ESCRT-I subunits<sup>58</sup>. Second, that Vps23p, Vps29p and Vps37p do not strictly depend on Mvb12p is validated by the findings that certain MVB sorting pathways, such as carboxypeptidase S (CPS) and Ste2 sorting, are effective even if Mvb12p is absent<sup>58,59</sup>. However, loss of function of Vps23p, Vps28p or Vps37p results in a complete block of the MVB pathway<sup>58</sup>. (c) Enrichment of negative genetic interactions in fan-in motif A-C pairs. The fraction of negative genetic interaction is defined as  $f = N_{neg}/(N_{neg} + N_{pos} + N_{noInteraction})$ .  $P$ -values in (a) and (c) were calculated with a one-tailed Fisher's exact test and visualized with an asterisk (\*) that stands for a  $P$ -value  $< 0.05$ .

by 50% when applying the evolutionary motif (from 23.5–35.8%; one-tailed Fisher's exact test;  $P = 0.00085$ ; Fig. 3c). It should be noted that this enrichment of negative genetic interactions is not owing to the functional complementation by homologous genes resulting from intra-complex gene duplications, as the results are hardly affected by removing homologous gene pairs (from 22.7–33.0%; one-tailed Fisher's exact test;  $P = 0.012$ ; Fig. 3c). As protein complexes are not necessarily active in standard laboratory conditions where genetic interactions have been measured, we expected that our test underestimates the predictive power. Indeed, when selecting for only protein complexes that are active in the cell (that is, B is essential) the predictive power even doubles (from 24.5–49.2%; one-tailed Fisher's exact test;  $P = 4.39 \times 10^{-5}$ ; Fig. 3c). Thus, the evolutionary model can predict protein pairs that have a negative genetic interaction significantly and substantially more often than random pairs from protein complexes. To further assess the performance of our model, we compared the prediction precision and sensitivity of it with a model by Pandey *et al.*<sup>18</sup> by mapping their results to the protein complexes. This model has the highest known prediction accuracy and is also independent on genetic interaction information as input. Interestingly, our model has a twofold higher prediction precision (precision—TruePositives/TruePositives + FalsePositives: 0.36 versus 0.18; sensitivity—TruePositives/TruePositives + FalseNegatives: 0.47 versus 0.78).

Notably, our model still has a precision of  $> 0.3$  when parameterized to the same sensitivity as Pandey's model (Supplementary Fig. S3).

In total, our model predicted 273 A-C pairs in evolutionary fan-in motifs in *S. cerevisiae* protein complexes, for most of which (60%) a genetic interaction has not been measured. However, to provide empirical evidence for the predicted negative interactions, we exploited available genetic interaction data in *Schizosaccharomyces pombe* and *Drosophila melanogaster* via orthology definitions from STRING7.0 (ref. 29). Following this approach, we found that for ten out of our A-C pairs a genetic interaction has been experimentally found in either in *S. pombe* or in *D. melanogaster* and, as expected, most cases (8/10) show a negative genetic interaction in those species (Supplementary Data 1).

**Negative genetic interactions reveal cancer drug targets.** The screen for negative genetic interactions has been shown to be a valuable strategy in the search for candidate cancer drug targets<sup>10,30</sup>. The common approach is to find proteins that have a negative genetic interaction with either an oncogene or a tumour-suppressor gene. As mutations in these genes cause cancer, the idea is that mutations in their negative genetic interaction partner would inhibit cancer cells to grow (that is, synthetic lethality) and leave normal cells relatively viable. Although a number of



promising examples have been reported to target cancer cells via synthetic lethality<sup>10,11,30</sup>, discovering genetic interactions by experimental approaches is very labour intensive. Therefore, we asked whether our model captures conserved genetic interactions between *S.cerevisiae* and other species like *D. melanogaster*, such that it can serve as a framework to establish genetic interactions for medical genetics. Based on the orthologue profiles from STRING7.0 (ref. 29), we found 90.1% (246 out of 273) of the predicted fan-in motifs in yeast are conserved in *D. melanogaster*, that is, all three genes in a fan-in motif are present in *D. melanogaster*. Of these, nine have been examined for genetic interaction in *D. melanogaster*<sup>31–33</sup>, and all show negative genetic interaction (note, 7/9 have also been found in *S.cerevisiae*). This suggests that our model can be used to predict negative genetic interactions in other species, such as mouse or human, which could provide a basis for prioritizing drug targets.

To achieve the highest coverage, we combined two strategies to predict cancer drug targets: (i) by using orthology mapping from predicted negative interactions from yeast to human and (ii) by a direct application of our model to human protein complexes<sup>34,35</sup>. By using orthologues of the genes in the predicted fan-in motifs in yeast, we predicted ~250 novel negative genetic interaction pairs in human, of which 36 involve a cancer-related gene (oncogene or tumour-suppressor gene)<sup>36</sup>. Notably, most of these pairs (83.4%, 30/36) have not been reported before as negative genetic interactions. To apply our method directly on human protein complexes<sup>34,35</sup>, we first trained our model with functional asymmetric enzyme pairs from the human genome-scale metabolic network<sup>37</sup> (see Methods). Then we used the model to predict negative genetic interaction pairs. Totally, we predicted 1,012 gene pairs with negative genetic interactions of which 57 involve a cancer-related gene. Thus, totally, we predicted 93 cases with cancer-related genes. The genes that have a negative genetic interaction with these cancer-related genes are potential drug

targets if they are essential in cancer cells while non-essential in normal cells. By examining gene essentiality in cancer cells<sup>38</sup> and non-essentiality in normal cells of *Mus musculus* (mouse), *D. melanogaster* or *Danio rerio* (zebrafish) (Supplementary Data 2), we found that 30 out of the 93 involve promising cancer drug targets (pink column in Fig. 4; Supplementary Data 2). Among these 30 prioritized targets, 20 have been found to be essential in at least one cancer type, that is, breast, ovary or pancreas, and non-essential in a model organism (pink column in Fig. 4). Interestingly, most of these predicted targets (16/20) are essential in the exact cancer type where their negative genetic interaction partners, the cancer-related genes, are reported to be mutated or overexpressed (blue column in Fig. 4; Supplementary Data 2). This empirical evidence suggests that the lethality of the cancer cells by knockdown of the predicted target gene is actually caused by a lethal double mutant of the predicted targets and the cancer-related gene. As expected, when considering only those cases for which essentiality is measured in cancer cells (that is, 60 + 18 cases, green column in Fig. 4), the predicted targets are more likely to be essential in cancer and non-essential in normal cells compared with non-motif gene pairs (fraction<sub>E\_cancer + NE\_normal</sub> = 0.26 versus 0.12, one-tailed Fisher's exact test;  $P = 4.8e - 04$ ). The remaining ten targets have not yet been experimentally examined for the essentiality in cancer cells: six are non-essential in *M. musculus* or *D. melanogaster* and four have not yet been measured (pink column in Fig. 4; Supplementary Data 2). Thus, we predicted 30 potential drug targets in total, that is, 20 with empirical support of essentiality in cancer cells and 10 novel ones (Table 1 and Supplementary Data 2). To give an example, one of the predicted drug targets, *TLE1*, has a negative genetic interaction with the cancer-related gene, *HDAC1* (ref. 39). *HDAC1* failed to be a direct drug target as the inhibition of mouse *Hdac1* caused embryonic lethality in normal development<sup>40</sup>. *TLE1*, on the other hand, has been found

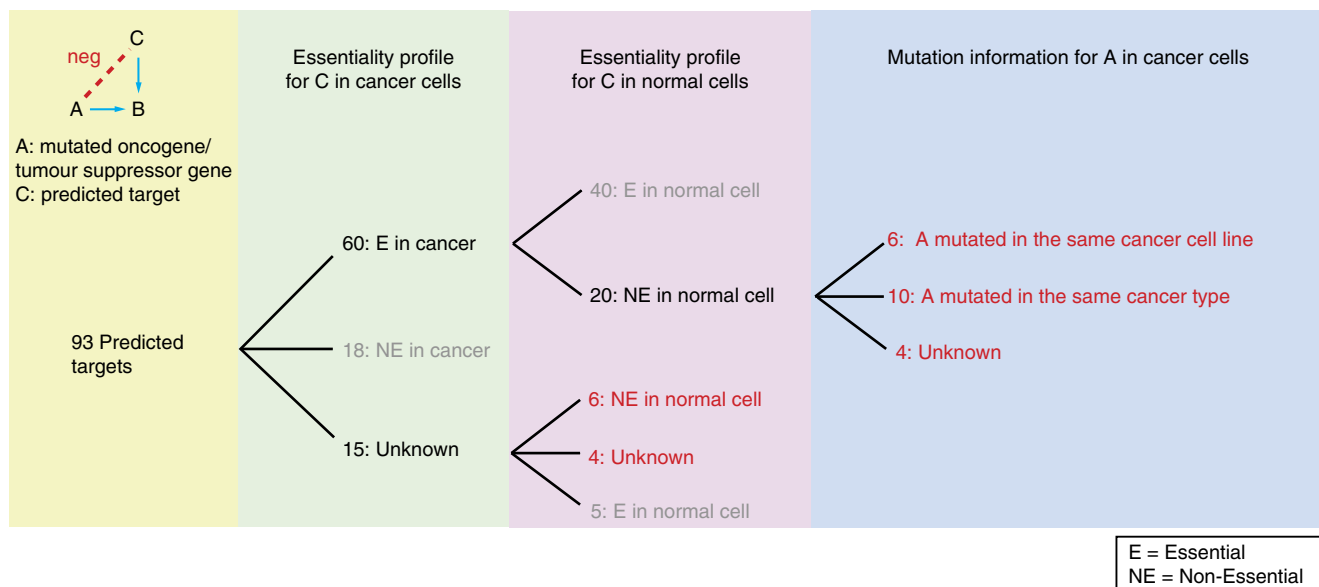


**Figure 4 | Prioritized cancer drug targets with empirical support.** Thirty prioritized cancer drug targets. The numbers in red represent the 30 promising targets. The numbers in grey represent the genes that failed to be targets as they are either non-essential in cancer cells or are essential in normal cells. In total, 93 genes are predicted to have a negative genetic interaction with a cancer-related gene. By examining gene essentiality in cancer and non-essentiality in normal cells, we prioritized 30 cancer drug targets. Twenty cases are essential in at least one cancer type, that is, breast, ovary or pancreas and non-essential in normal cells. Experimentally detected genetic variation/overexpression of the cancer-related gene and the RNA interference of the predicted targets in the same cancer type or the same cancer cell line were combined suggesting a double mutant. For most of these (16/20), there is empirical evidence that the cancer-related gene is mutated in either the same cancer type or the same cancer cell line as the predicted targets (blue column). For six cases that are confirmed to be non-essential in normal cells, the essentiality in cancer still needs to be examined experimentally. For four cases, the essentiality in both cancer cells and normal cells is not yet measured (red numbers in the pink column).

**Table 1 | List of predicted cancer drug targets.**

Cancer-related genes	Predicted target genes with empirical evidence: essential in cancer cell non-essential in normal cell	Novel predicted target genes: *unknown essentiality in normal cell and cancer cell **non-essential in normal cell and unknown essentiality in cancer cell
DDB2 FBXW7 EML4	LSMD1 HDACS HDAC6 PPWD1 PPIH PPIE KIAA0564 NSUN2 NSUN5	PPIB PPIC PPID** NTG1 GNL3L SSTR5**
BCL3 NOTCH2 CDKN2C NFKB2	HDACS HDAC6 PPWD1 PPIH PPIE	PPIB PPIC PPID**
MSI2 CREBBP EP300 BRD4  PBRM1 BRD3 TRI-M24 SMARCA4	DENR USP12 USP22 USP30	USP45**
PIK3CA HDAC1 DDX5 DDX6 DDX10 EIF4A2	USP12 USP22 USP30 TLE1	USP45** ATAD2*
PBRM1 MED12 HIST1H4I EZH2 RPN1 PIK3R1 SMAD4 CCNE1 CREBBP FANCF FANCC FANCF SEPT9	ACTG1 MED14 H3F3A EED MAGT1 ESR1 JUND SKP1 KAT2B	C17orf70* FANCB* FANCB* SEPT11**

Twenty predicted cancer drug targets with experimental evidence (second column) and ten novel targets (third column). The grey-shaded rows show targets predicted by using orthology mapping and the rows without show targets predicted directly from human protein complexes. Each grey-shaded cell represents a Clusters of Orthologous Group (COG) of cancer-related genes or predicted drug targets. The first column shows the cancer-related genes. The second column shows 20 predicted drug targets with empirical evidence where each gene is essential in at least one cancer cell and non-essential in model organisms. The third column shows ten novel targets for which the essentiality in cancer cells has not yet been measured.

to be essential in several types of cancer cells<sup>38</sup> and non-essential in *D. melanogaster*<sup>41</sup>. In addition, *TLE1* and *HDAC1* have a confirmed negative genetic interaction in *D. melanogaster*<sup>41</sup>, which makes *TLE1* a promising drug target for further analysis.

Another example is the predicted interaction between *NSUN2* and *FBXW7* (Fig. 5). *NSUN2* is experimentally found to be essential in cancer cells<sup>42</sup>, and *FBXW7*, a tumour-suppressor gene, has been found to be mutated in cancer cells<sup>43</sup>. In normal cells, *NSUN2* and *FBXW7* both function to regulate cellular differentiation via two different mechanisms. *FBXW7* regulates cell differentiation by inhibiting *c-Myc*<sup>44</sup> and proteins in Notch pathway<sup>45</sup>, and *NSUN2* functions to maintain normal cell differentiation when activated by *LEF1/β-catenin* complex, which is part of *Wnt* pathway<sup>46,47</sup>. It has been found that the loss of *FBXW7* results in elevated expression of *c-Myc*<sup>44</sup>, which results in an upregulation of *NSUN2* (ref. 48). As a result, *NSUN2* stabilizes the mitotic spindle in fast cell proliferation in cancer cell growth<sup>42</sup>. Thus, targeting *NSUN2* can kill cancer cells while leaving normal cells relatively unaffected, owing to the compensatory *FBXW7*-Notch pathway. This is further supported by the non-essentiality of *NSUN2* in normal mouse model<sup>47</sup>.

**Discussion**

Even though various experimental techniques are available to study protein function, understanding their functions within protein complexes and their relationships between each other in a complex remains a challenge. Here, we have developed a model to predict functional relationships within protein complexes using the evolutionary history of genomes in terms of gene gain and

loss events. We first focused on the relationships in which the function of one protein A depends on the function of another protein B, but in which the reverse relationship is much weaker. We predicted such asymmetry by integrating various evolutionary scenarios, such as, gene B is more frequently gained across evolutionary history in the absence of gene A than *vice versa*. So, B can occur without A, but A cannot occur without B. To validate the method, we showed that the predicted functional asymmetry is consistent with various sources of empirical evidence, such as asymmetry in gene essentiality and single-knockout growth defects. However, one-third of the gene pairs in the same complex with asymmetry in gene essentiality (633/2,130) have not been captured by our model. Perfect prediction can, however, not be expected, because it is strictly based on complete gene loss and gain. Our model may therefore benefit from more fine-scale evolutionary events, such as the incorporation of mutation rates. Thus, in species where both A and B are still present, there might be asymmetry in the extent to which they have diverged at the sequence level from their respective ancestors. Second, the essentiality and growth defect data sets<sup>4,49</sup> cover specific nutrient environments, which might not be experienced by species in our evolutionary model. Such differences in physiological conditions may result in different genome evolution and, as such, it could negatively affect model predictions.

Interestingly, functional asymmetric relationships can be used to predict negative genetic interactions in those cases where multiple proteins, for instance, A and C, have asymmetry with the same protein B. The underlying idea is that functional asymmetry is owing to the fact that A and C can compensate for each other's absence. Indeed, we have shown that our model increases the



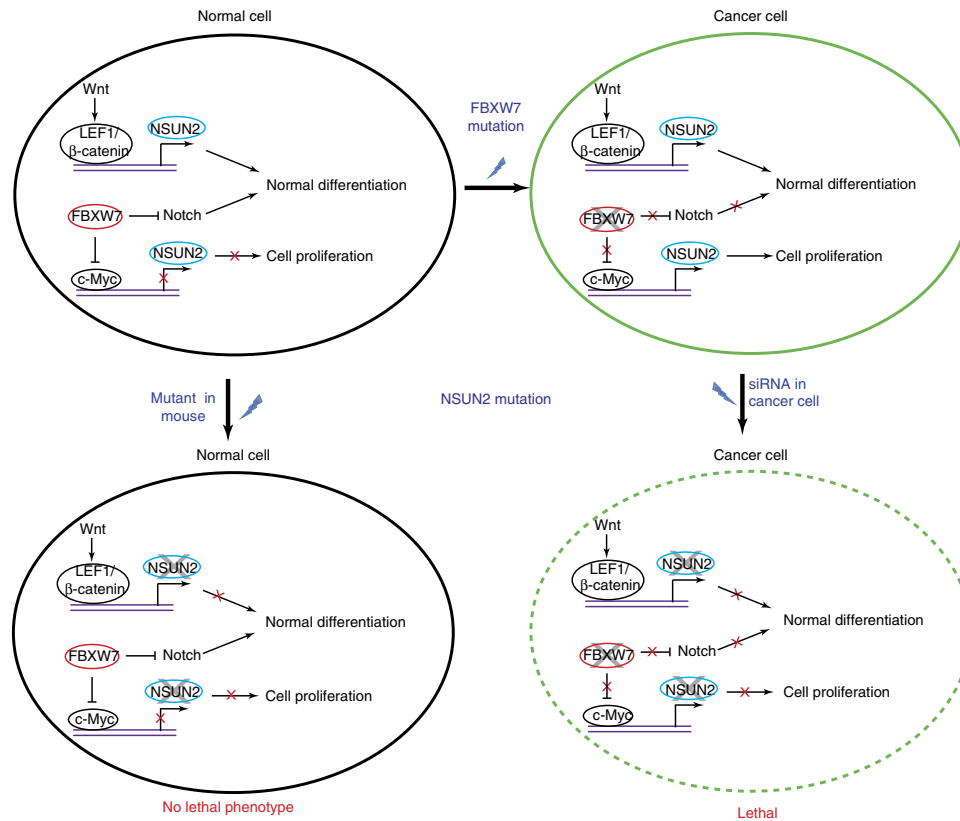


**Figure 5 | A cancer drug target revealed by predicted negative genetic interactions.** *NSUN2* is predicted to have a negative genetic interaction with *FBXW7*. Targeting *NSUN2* can kill the cancer cells while leaving the normal cell relatively unaffected. In normal cells, the tumour-suppressor gene *FBXW7* has functional redundancy with *NSUN2* in regulating cellular differentiation. In cancer cells, loss of function of *FBXW7* results in an elevated expression of *c-Myc*. Activation of *c-Myc* results in the upregulation of *NSUN2* that is essential for cell proliferation. Owing to a synthetic lethality between *FBXW7* and *NSUN2*, targeting *NSUN2* kills cancer cells, while leaving normal cells relatively unaffected. A solid line represents an active protein, for example, *FBXW7* inhibiting the accumulation of *NOTCH1* and *NOTCH3* in normal cells<sup>45</sup>. A red cross illustrates the disruption of the function of a protein, that is, transcriptional regulation of *NSUN2* by *c-Myc2* is repressed in normal cell, or the disruption of a cellular function, that is, differentiation or proliferation.

predictive power for negative genetic interactions in *S. cerevisiae* protein complexes by 50–100% relative to random protein pairs from the same complex. Moreover, we predict many novel genetic interactions, of which eight have been experimentally verified in *S. pombe* and *D. melanogaster*. Although this number is not high, this is not unexpected given that genome-scale genetic interaction screens have only been performed in *S. cerevisiae*<sup>20</sup> and *S. pombe*<sup>50</sup>. Moreover, only one screen under standard nutrient condition has been conducted for these two species, respectively, and it remains to be seen how genetic interactions vary across other nutrient conditions. It would therefore be interesting to apply our model to study the variation of interactions across conditions, for example, to re-evaluate evolutionary theories that are based on adaptive landscapes (for example, robustness against mutations in single environments) initialized by studies on metabolism<sup>51</sup>. One strategy would be to integrate gene expression profiles across a wide range of nutrient conditions with protein complex data to remove unexpressed subunits from protein complexes and thus obtain condition-specific complexes. In addition, condition-specific essentiality profiles<sup>4</sup> could be used to constrain the independent protein (B) to be essential. As a result, one could predict fan-in motifs that are specific for a given condition. Our finding that the predictive power of negative genetic interactions doubles when incorporating essentiality supports such a strategy.

Various recent studies have stated that the discovery of (negative) genetic interactions is a very important step towards a

full understanding of the genetic basis of complex diseases and providing a framework to discover drug targets<sup>52–54</sup>. Even though there are a number of very promising candidate drug targets discovered by using genetic interactions<sup>10,11</sup>, effectively identifying them experimentally remains a major challenge. In contrast to other prediction models<sup>12,13,18</sup>, our model does not depend on genetic interaction screens, which are available in a very limited number of species. Thus, our model can be applied to predict genetic interactions in species even when no empirical genetic interaction information is available. Moreover, compared with Pandey *et al.*<sup>18</sup>, our model has a significantly higher prediction precision. Our approach is therefore useful to prioritize drug candidates. We found 20 cancer drug targets for which there is empirical evidence that they are essential in tumour cells and predicted ten novel drug targets. Notably, the majority (25/30) has not been measured in yeast or predicted by other computational approaches<sup>13,18</sup>. These targets are promising given the empirical evidence that all are essential in at least one cancer type, such as breast, pancreas or ovarian cancer, while non-essential in model organisms. Future studies should reveal to what extent these targets are (i) non-essential in the same human healthy cell type, (ii) conserved across different tumour types and (iii) vulnerable for drug compounds.

In the light of medical genetics, the presented approach can be applied to mammals when future protein–protein interaction networks become available for cancer and normal cell lines. This would allow for more specific predictions of cancer drug targets.

It should be noted that although we focused on protein complexes, our model might be used to predict interactions for any gene pair, as long as they are known to have a functional relationship between them. Taken together, this study shows that negative genetic interactions in protein complexes can be predicted by genome evolution, which has an application in searching for drug targets and in understanding human diseases.

## Methods

**Protein complexes.** Four hundred and nine and 2,468 protein complexes of *S. cerevisiae*<sup>17</sup> and human<sup>34,35</sup> were used to predict negative genetic interactions within them, respectively. For each protein complex, all pair-wise combinations of proteins were generated as input for our evolutionary model.

**Reconstruction of ancestral states.** We used the presence and absence of orthologous genes across 373 species obtained from STRING 7.0 orthologous groups<sup>29</sup> to reconstruct ancestral states of genes. We inferred the most parsimonious ancestral presence/absence states of each gene by using a rooted trifurcation (Achaea/Eukaryote/Eubacteria) phylogenetic tree of 373 species. All results were obtained using a gain/loss cost ratio of 2/1 and a delayed transition assumption (DELTRAN) in PAUP<sup>55</sup>. From the ancestral state reconstruction, we generated 11 evolutionary variables as inputs to the following classification step. The integration of these 11 evolutionary variables gives the highest correct classification rate compared with alternative integrations of evolutionary variables.

For each gene pair A–B, we examined the following six evolutionary scenarios: (i) both genes were absent in the ancestor (a) and one was gained in the descendant (d) (a00\_d10 or a00\_d01), (ii) the presence of only one gene in the ancestor was maintained in the descendant (a10\_d10 or a01\_d01), (iii) both genes were present in the ancestor and one was lost in the descendant (a11\_d01 or a11\_d10), (iv) a gain of one gene occurred when the other was present in the ancestor (a01\_d11 or a10\_d11), (v) only one gene was present in the ancestor and was lost in the descendant (a10\_d00 or a01\_d00) and (vi) only one gene was present in the ancestor and was lost in the descendant while the other gene was gained (a10\_d01 or a01\_d10) (Fig. 2b).

For gene A, we also calculated five fractions that reflect evolutionary asymmetry between A and B,  $f_1$ :  $a11\_d01/(a11\_d01 + a11\_d10)$ ,  $f_2$ :  $a01\_d11/(a01\_d11 + a10\_d11)$ ,  $f_3$ :  $a01\_d01/(a01\_d01 + a10\_d10)$ ,  $f_4$ :  $a01\_d11/(a01\_d11 + a00\_d10)$  and  $f_5$ :  $a01\_d11*[a01\_d11 - a00\_d10 + 1]/[a01\_d11 + a00\_d10]$ .

**Evolutionary information to predict asymmetry of gene pairs.** First, we reconstructed ancestral states for 2,400 directionally coupled enzyme pairs (functional asymmetry; A → B) in the yeast metabolic network<sup>19</sup> and generated the 11 evolutionary variables. Directional coupling was found by constraining the reaction flux of one to a finite value followed by minimizing and maximizing another, and *vice versa*<sup>14</sup>. A → B is found when the minimum flux through A is zero while the maximum is a finite value (when constraining B to a finite flux), and the minimum and maximum flux through B is unequal to zero when A is constrained to a finite value. Thus, the activity of A depends on the activity of B, but not the reverse (A → B). Each of the 11 evolutionary variables is a predictor for functional asymmetry between an enzyme pair (A → B) as the 11 variables of a dependent A differ from those of an independent B. More specifically, for evolutionary events (i) and (ii), A is expected to occur less often than the independent B. For the other four evolutionary events, A is expected to occur more often than the independent B. Furthermore, we expect  $f_1$ ,  $f_2$ ,  $f_3$  and  $f_4$  to be larger than 0.5, and  $f_5$  to be larger than 0 for asymmetric functional relationships (Supplementary Fig. S1).

Given the fact that these 11 variables are not independent from each other, we used a Tree Augmented Naïve Bayes (TAN) classifier to integrate these predictors. The TAN classifier relaxes the assumption of independence of input variables. The classifier is trained on the 2,400 directionally coupled enzyme pairs using WEKA<sup>56</sup>. The classifier estimates conditional probabilities of one gene being independent ( $\alpha_1$ ) or dependent ( $\alpha_2$ ), where  $\alpha_1 + \alpha_2 = 1$ . The gene is predicted to be either independent (if  $\alpha_1 > \alpha_2$ ) or dependent (if  $\alpha_1 < \alpha_2$ ) with a conditional probability ( $\alpha$ ), where  $\alpha = \max(\alpha_1, \alpha_2)$ . To predict the functional relationship in protein complexes by this classifier, we first reconstructed ancestral states for 8,711 protein pairs (A–B) and generated the 11 evolutionary variables for A and B. The functional relationship of A–B is determined as follows: (i) the classifier generates class predictions for A with a probability estimate ( $\alpha$ ); (ii) identifying predictions with high confidence by a cutoff on  $\alpha$  (any prediction where  $\alpha$  is smaller than the cutoff remains unclassified); (iii) protein B is predicted in the same way; and (iv) combining the classification result of A and B, A–B is predicted as functionally asymmetric when A is dependent and B is independent or *vice versa*. Otherwise, there is no evidence for functional asymmetry and the pair becomes unclassified (Fig. 2c).

**Gene essentiality.** Essentiality data were obtained from MIPS database<sup>49</sup>. If a gene is annotated as both essential and non-essential in different sources, the essentiality is assigned according to the majority rule. Otherwise, a gene was marked as ambiguous.

For predicted asymmetric pairs (A → B), we counted cases where only B is essential ( $n_{01}$ ) and cases where only A is essential ( $n_{10}$ ). For symmetric pairs (A–B), it is expected that  $n_{01}$  is equal to  $n_{10}$ . To test against the null hypothesis of no relationship between predicted functional asymmetry and asymmetry in essentiality, we subjected the  $2 \times 2$  contingency table of essential/non-essential versus symmetric/asymmetric to a one-tailed Fisher's exact test.

**Growth defect of single-gene knockouts in rich medium.** Growth defect of single-gene knockouts was obtained from two studies<sup>20,21</sup>, which cover 75% of all genes in *S. cerevisiae*. A growth defect was considered as substantial if a gene knockout causes a growth defect > 10% (ref. 4).

For predicted asymmetric pairs with two non-essential genes (A → B), we counted cases where knockout of B causes a more severe growth defect ( $n_{01}$ ) and cases where knockout of A causes a more severe growth defect ( $n_{10}$ ). For functional symmetric pairs (A–B), it is expected that  $n_{01}$  is equal to  $n_{10}$ . To test against the null hypothesis of no relationship between predicted functional asymmetry and asymmetry in growth defect, we subjected the  $2 \times 2$  contingency table of  $n_{01}/n_{10}$  versus symmetric/asymmetric to a one-tailed Fisher's exact test.

**Negative genetic interactions in the metabolic network.** We obtained fan-in motif A–C pairs for metabolic reactions (Fig. 1c) by using flux coupling between enzymes within the genome-scale metabolic network of *S. cerevisiae* (see above). The fan-in motif A–C pairs have two characteristics: (i) A and C both depend on a third essential protein B (A → B and C → B) and (ii) the A–C pair is uncoupled. For experimental validation, we used an empirical genetic interaction profile from Szappanos *et al.* (obtained from the Supplementary Information<sup>21</sup>). If no significant genetic information was available for a pair of genes, we determined it as not measured and excluded it from the analysis.

To test against the null hypothesis of no enrichment of negative genetic interactions in fan-in motif A–C pairs, we summarized the motif A–C/non-motif A–C pairs versus with/without negative genetic interaction in a  $2 \times 2$  contingency table and subjected it to a one-tailed Fisher's exact test.

**Negative genetic interactions in protein complexes.** We obtained A–C pairs with evolutionary fan-in motifs (Fig. 1a) from asymmetric functional relationships predicted by the TAN model (Fig. 2c). The evolutionary fan-in motif is characterized by (i) A and C depend on B, but not *vice versa* and (ii) A does not depend on C and *vice versa*. To ensure A–C is not an asymmetric pair, we applied the cutoff for significant functional asymmetry to  $\alpha > = 0.7$ . At this cutoff, the correct classification rate increases the most at the smallest cost of samples size (Supplementary Fig. S4).

Genetic interaction data were obtained from BioGRID<sup>31</sup>. As BioGRID does not specify whether the genetic interaction of a gene pair has been measured, we integrated the original data from nine high-throughput data sets<sup>20–28</sup>, to generate a list of measured genetic interactions (either positive, negative or no interaction). If a pair of genes has both a negative and a positive genetic interaction, the genetic interaction was assigned according to the majority rule.

To test against the null hypothesis of no enrichment of negative genetic interactions in pairs with a fan-in motif, we summarized motif A–C/non-motif A–C versus with/without negative genetic interaction in a  $2 \times 2$  contingency table and tested using a one-tailed Fisher's exact test.

**Prediction of cancer drug targets.** We mapped predicted negative genetic interactions from yeast to human via orthology from STRING7.0 (ref. 29). To retrieve drug targets, we first mapped cancer gene information from the Cancer Genome Project<sup>36</sup> to the predicted genetic interactions to extract predictions involving one oncogene or tumour-suppressor gene. Then we mapped gene essentiality measurements in cancer from Marcotte *et al.*<sup>38</sup> to the predictions. In addition, non-essentiality of the drug targets in normal cells/tissues was examined by literature mining covering *M. Musculus*, *D. melanogaster* or *D. rerio*.

To predict targets directly from human protein complexes, we trained our model on functional asymmetric enzyme pairs from the human genome-scale metabolic network<sup>37</sup> via Flux Coupling Analysis (see also above for yeast and Burgard *et al.*<sup>14</sup>). Subsequently, we used experimentally determined protein complexes<sup>34,35</sup> to predict human-specific negative genetic interactions via the evolutionary fan-in motifs. Finally, we examined gene essentiality among predicted drug targets in cancer and normal cells/tissues as outlined above.

## References

1. Badano, J. L. & Katsanis, N. Beyond Mendel: an evolving view of human genetic disease transmission. *Nat. Rev. Genet.* **3**, 779–789 (2002).
2. Moore, J. H. The ubiquitous nature of epistasis in determining susceptibility to common human diseases. *Hum. Hered.* **56**, 73–82 (2003).
3. Gavin, A. C. *et al.* Proteome survey reveals modularity of the yeast cell machinery. *Nature* **440**, 631–636 (2006).
4. Giaever, G. *et al.* Functional profiling of the *Saccharomyces cerevisiae* genome. *Nature* **418**, 387–391 (2002).
5. Krogan, N. J. *et al.* Global landscape of protein complexes in the yeast *Saccharomyces cerevisiae*. *Nature* **440**, 637–643 (2006).

6. Ideker, T. & Krogan, N. J. Differential network biology. *Mol. Syst. Biol.* **8**, 565 (2012).
7. Dirick, L. & Nasmyth, K. Positive feedback in the activation of G1 cyclins in yeast. *Nature* **351**, 754–757 (1991).
8. Richardson, H. E., Wittenberg, C., Cross, F. & Reed, S. I. An essential G1 function for cyclin-like proteins in yeast. *Cell* **59**, 1127–1133 (1989).
9. Mani, S. R., Onge, R. P., Hartman, J. L., Giaever, G. & Roth, F. P. Defining genetic interaction. *Proc. Natl Acad. Sci. USA* **105**, 3461–3466 (2008).
10. Weidle, U. H., Maisel, D. & Eick, D. Synthetic lethality-based targets for discovery of new cancer therapeutics. *Cancer Genomics Proteomics* **8**, 159–171 (2011).
11. Muller, F. L. *et al.* Passenger deletions generate therapeutic vulnerabilities in cancer. *Nature* **488**, 337–342 (2012).
12. Paladugu, S., Zhao, S., Ray, A. & Raval, A. Mining protein networks for synthetic genetic interactions. *BMC Bioinform.* **9**, 426 (2008).
13. Wong, S. L. *et al.* Combining biological networks to predict genetic interactions. *Proc. Natl Acad. Sci. USA* **101**, 15682–15687 (2004).
14. Burgard, A. P., Nikolaev, E. V., Schilling, C. H. & Maranas, C. D. Flux coupling analysis of genome-scale metabolic network reconstructions. *Genome Res.* **14**, 301–312 (2004).
15. Notebaart, R., Kensche, P., Huynen, M. & Dutilh, B. Asymmetric relationships between proteins shape genome evolution. *Genome Biol.* **10**, R19 (2009).
16. Bowers, P. M., Cokus, S. J., Eisenberg, D. & Yeates, T. O. Use of logic relationships to decipher protein network organization. *Science* **306**, 2246–2249 (2004).
17. Benschop, J. J. *et al.* A consensus of core protein complex compositions for *Saccharomyces cerevisiae*. *Mol. Cell.* **38**, 916–928 (2010).
18. Pandey, G. *et al.* An integrative multi-network and multi-classifier approach to predict genetic interactions. *PLoS Comput. Biol.* **6**, e1000928 (2010).
19. Kuepfer, L., Sauer, U. & Blank, L. M. Metabolic functions of duplicate genes in *Saccharomyces cerevisiae*. *Genome Res.* **15**, 1421–1430 (2005).
20. Costanzo, M. *et al.* The genetic landscape of a cell. *Science* **327**, 425–431 (2010).
21. Szappanos, B. *et al.* An integrated approach to characterize genetic interaction networks in yeast metabolism. *Nat. Genet.* **43**, 656–662 (2011).
22. Aguilar, P. S. *et al.* A plasma-membrane E-MAP reveals links of the eisosome with sphingolipid metabolism and endosomal trafficking. *Nat. Struct. Mol. Biol.* **17**, 901–908 (2010).
23. Bandyopadhyay, S. *et al.* Rewiring of genetic networks in response to DNA damage. *Science* **330**, 1385–1389 (2010).
24. Collins, S. R. *et al.* Functional dissection of protein complexes involved in yeast chromosome biology using a genetic interaction map. *Nature* **446**, 806–810 (2007).
25. Fiedler, D. *et al.* Functional organization of the *S. cerevisiae* phosphorylation network. *Cell* **136**, 952–963 (2009).
26. Schuldiner, M. *et al.* Exploration of the function and organization of the yeast early secretory pathway through an epistatic miniarray profile. *Cell* **123**, 507–519 (2005).
27. Wilmes, G. M. *et al.* A genetic interaction map of rna-processing factors reveals links between Sem1/Dss1-containing complexes and mRNA export and splicing. *Mol. Cell.* **32**, 735–746 (2008).
28. Zheng, J. *et al.* Epistatic relationships reveal the functional organization of yeast transcription factors. *Mol. Syst. Biol.* **6**, 420 (2010).
29. von Mering, C. *et al.* STRING 7—recent developments in the integration and prediction of protein interactions. *Nucleic Acids Res.* **35**, D358–D362 (2007).
30. Reinhardt, H. C., Jiang, H., Hemann, M. T. & Yaffe, M. B. Exploiting synthetic lethal interactions for targeted cancer therapy. *Cell Cycle* **8**, 3112–3119 (2009).
31. Stark, C. *et al.* The BioGRID Interaction Database: 2011 update. *Nucleic Acids Res.* **39**, D698–D704 (2011).
32. Horn, T. *et al.* Mapping of signaling networks through synthetic genetic interaction analysis by RNAi. *Nat. Meth.* **8**, 341–346 (2011).
33. McQuilton, P., St Pierre, S. E., Thurmond, J. & Consortium, t. F. FlyBase 101 – the basics of navigating FlyBase. *Nucleic Acids Res.* **40**, D706–D714 (2012).
34. Havugimana, Pierre C. *et al.* A census of human soluble protein complexes. *Cell* **150**, 1068–1081 (2012).
35. Ruepp, A. *et al.* CORUM: the comprehensive resource of mammalian protein complexes—2009. *Nucleic Acids Res.* **38**, D497–D501 (2010).
36. Futreal, P. A. *et al.* A census of human cancer genes. *Nat. Rev. Cancer* **4**, 177–183 (2004).
37. Duarte, N. C. *et al.* Global reconstruction of the human metabolic network based on genomic and bibliomic data. *Proc. Natl Acad. Sci. USA* **104**, 1777–1782 (2007).
38. Marcotte, R. *et al.* Essential gene profiles in breast, pancreas and ovarian cancer cells. *Cancer Discov.* **2**, 172–189 (2012).
39. Lagger, G. *et al.* The tumor suppressor p53 and histone deacetylase 1 are antagonistic regulators of the cyclin-dependent kinase inhibitor p21/WAF1/CIP1 gene. *Mol. Cell. Biol.* **23**, 2669–2679 (2003).
40. Lagger, G. *et al.* Essential function of histone deacetylase 1 in proliferation control and CDK inhibitor repression. *EMBO J.* **21**, 2672–2681 (2002).
41. Chen, G., Fernandez, J., Mische, S. & Courey, A. J. A functional interaction between the histone deacetylase Rpd3 and the corepressor Groucho in *Drosophila* development. *Genes Dev.* **13**, 2218–2230 (1999).
42. Hussain, S. *et al.* The nucleolar RNA methyltransferase Misu (NSun2) is required for mitotic spindle stability. *J. Cell. Biol.* **186**, 27–40 (2009).
43. Welcker, M. & Clurman, B. E. FBW7 ubiquitin ligase: a tumour suppressor at the crossroads of cell division, growth and differentiation. *Nat. Rev. Cancer* **8**, 83–93 (2008).
44. Welcker, M. *et al.* The Fbw7 tumor suppressor regulates glycogen synthase kinase 3 phosphorylation-dependent c-Myc protein degradation. *Proc. Natl Acad. Sci. USA* **101**, 9085–9090 (2004).
45. Matsumoto, A. *et al.* Fbxw7-dependent degradation of notch is required for control of “stemness” and neuronal-glial differentiation in neural stem cells. *J. Biol. Chem.* **286**, 13754–13764 (2011).
46. Hirabayashi, Y. *et al.* The Wnt/ $\beta$ -catenin pathway directs neuronal differentiation of cortical neural precursor cells. *Development* **131**, 2791–2801 (2004).
47. Blanco, S. *et al.* The RNA-methyltransferase Misu (NSun2) poises epidermal stem cells to differentiate. *PLoS Genet.* **7**, e1002403 (2011).
48. Frye, M. & Watt, F. M. The RNA methyltransferase Misu (NSun2) mediates Myc-induced proliferation and is upregulated in tumors. *Curr. Biol.* **16**, 971–981 (2006).
49. Mewes, H. W. *et al.* MIPS: analysis and annotation of proteins from whole genomes. *Nucleic Acids Res.* **32**, D41–D44 (2004).
50. Frost, A. *et al.* Functional repurposing revealed by comparing *S. pombe* and *S. cerevisiae* genetic interactions. *Cell* **149**, 1339–1352 (2012).
51. Harrison, R., Papp, B., Pál, C., Oliver, S. G. & Delneri, D. Plasticity of genetic interactions in metabolic networks of yeast. *Proc. Natl Acad. Sci. USA* **104**, 2307–2312 (2007).
52. Fedele, S. V. *et al.* A genetic interaction network of five genes for human polycystic kidney and liver diseases defines polycystin-1 as the central determinant of cyst formation. *Nat. Genet.* **43**, 639–647 (2011).
53. Lanson, N. A. *et al.* A *Drosophila* model of FUS-related neurodegeneration reveals genetic interaction between FUS and TDP-43. *Hum. Mol. Genet.* **20**, 2510–2523 (2011).
54. Willis, M. S. *et al.* Functional redundancy of SWI/SNF catalytic subunits in maintaining vascular endothelial cells in the adult heart. *Circ. Res.* **111**, e111–e122 (2012).
55. Swofford, D. L. PAUP\* Phylogenetic Analysis Using Parsimony (\*and Other Methods). Version 4. (Sinauer Associates, Sunderland, Massachusetts, 2003).
56. Hall, M. *et al.* The WEKA Data Mining Software: An Update Volume 11, Issue 1SIGKDD Explorations, 2009).
57. Kostelansky, M. S. *et al.* Molecular architecture and functional model of the complete yeast ESCRT-I heterotetramer. *Cell* **129**, 485–498 (2007).
58. Curtiss, M., Jones, C. & Babst, M. Efficient cargo sorting by ESCRT-I and the subsequent release of ESCRT-I from multivesicular bodies requires the subunit Mvb12. *Mol. Biol. Cell* **18**, 636–645 (2007).
59. Oestreich, A. J., Davies, B. A., Payne, J. A. & Katzmam, D. J. Mvb12 is a novel member of ESCRT-I involved in cargo selection by the multivesicular body pathway. *Mol. Biol. Cell* **18**, 646–657 (2007).

## Acknowledgements

This work was supported by The BioRange programme of The Netherlands Bioinformatics Centre (NBIC), supported by a BSK grant through The Netherlands Genomics Initiative (NGI). R.A.N. is supported by The Netherlands Organisation for Scientific Research (NWO–VENI Grant).

## Author contributions

X.L., P.R.K., M.A.H. and R.A.N. conceived and designed the study. X.L. performed the analyses. X.L., M.A.H. and R.A.N. wrote the manuscript.

## Additional information

**Supplementary Information** accompanies this paper at <http://www.nature.com/naturecommunications>

**Competing financial interests:** The authors declare no competing financial interests.

**Reprints and permission** information is available online at <http://npg.nature.com/reprintsandpermissions/>

**How to cite this article:** Lu, X. *et al.* Genome evolution predicts genetic interactions in protein complexes and reveals cancer drug targets. *Nat. Commun.* 4:2124 doi: 10.1038/ncomms3124 (2013).



This work is licensed under a Creative Commons Attribution-NonCommercial-NoDerivs 3.0 Unported License. To view a copy of this license, visit <http://creativecommons.org/licenses/by-nc-nd/3.0/>